Relativistic description of magnetic moments in nuclei with doubly closed shells plus or minus one nucleon

J. Li (李剑),[1] J. X. Wei (韦霁轩),[2] J. N. Hu (胡金牛),[3] P. Ring,[3,4] and J. Meng (孟杰)[2,3,5,*]

[1]*College of Physics, Jilin University, Changchun 130012, China*

[2]*School of Physics and Nuclear Energy Engineering, Beihang University, Beijing 100191, China*

[3]*State Key Laboratory of Nuclear Physics and Technology, School of Physics, Peking University, Beijing 100871, China*

[4]*Physik Department, Technische Universität München, D-85747 Garching, Germany*

[5]*Department of Physics, University of Stellenbosch, Stellenbosch, South Africa*

(Received 1 July 2013; revised manuscript received 22 September 2013; published 6 December 2013)

Using the relativistic point-coupling model with the density functional PC-PK1, the magnetic moments of the nuclei ^{207}Pb, ^{209}Pb, ^{207}Tl, and ^{209}Bi with a jj closed-shell core ^{208}Pb are studied on the basis of relativistic mean field theory. The corresponding time-odd fields, the one-pion exchange currents, and the first- and second-order corrections are taken into account. The present relativistic calculations are in reasonable agreement with the data. The relative deviation between theory and experiment for these four nuclei is 6.1% for the relativistic calculations and somewhat smaller than the value of 13.2% found in earlier nonrelativistic investigations. It turns out that the pion meson is important for the description of magnetic moments, first by means of one-pion exchange currents and second by the residual interaction provided by the pion exchange.

DOI: 10.1103/PhysRevC.88.064307 PACS number(s): 21.10.Ky, 21.30.Fe, 21.60.Jz, 27.80.+w

I. INTRODUCTION

The nuclear magnetic moment is an important observable in nuclear physics. It provides rich information about nuclear structure, serves as a stringent test of nuclear models, and has attracted the attention of nuclear physicists since the early days [1–4]. The theoretical description of nuclear magnetic moments has been a long-standing problem. In the past few decades, many successful nuclear structure models have been developed. However, the application of these models for nuclear magnetic moments is still not satisfactory.

In the extreme single-particle shell model, the magnetic moment of an odd-A nucleus is carried only by one valence nucleon (valence-nucleon approximation), which leads to the well-known Schmidt values. It was observed in the early 1950s [5], however, that almost all nuclear magnetic moments are sandwiched between the two Schmidt lines [6]. Therefore, considerable efforts have been made to explain the deviations of the nuclear magnetic moments from the Schmidt values, which can be contributed from meson exchange current (MEC, i.e., the exchange of a charged meson) and configuration mixing (CM, or core polarization, i.e., the correlation not included in the mean-field approximation) [7–9].

In 1954, Arima and Horie [10] pointed out a very distinct difference between the following two groups of nuclei: The cores of the nuclei in the first group (^{16}O and ^{40}Ca cores) are LS closed, i.e., the spin-orbit partners $j = l \pm \frac{1}{2}$ of the core are completely occupied. Therefore they are expected not to be excited strongly by an external field with $M1$ character. On the other hand, the cores of the nuclei in the second group (such as ^{208}Pb) are jj closed, i.e., one of the spin-orbit partners is open, and an $M1$ external field can strongly excite core nucleons to the empty spin-orbit partner. This $M1$ giant resonance state of the core can be momentary excited by the interaction with the valence nucleon. This is the idea of first-order configuration mixing, which is also called the Arima-Horie effect [11]. It explains not only the difference between these two groups of nuclei but also deviations of magnetic moments from the Schmidt lines for many nuclei [10,12,13].

In the late 1960s, it became clear after many calculations that the first-order effect is not enough to explain the large deviations from the Schmidt values in high spin states, especially ^{209}Pb. Pion exchange is very important to understand nuclear magnetic moments, as was first pointed out by Miyazawa in 1951 [14] and by Villars in 1952 [15]. This correction changes the gyromagnetic ration of orbital angular momentum of a nucleon in the nucleus [16] and improves the agreement between theoretical and observed values [17]. Furthermore, second-order configuration mixing had been taken into account first in Refs. [18–20], and this was also important for understanding the deviations as well as meson exchange current [21,22].

In the past decades, relativistic mean field (RMF) theory has been successfully applied to the analysis of nuclear structure over the whole periodic table, from light to superheavy nuclei with a few universal parameters [23–26]. However, relativistic descriptions of nuclear magnetic moments are mostly restricted to LS closed-shell nuclei ± 1 nucleon. It has been known for some time that in straightforward applications of the relativistic single-particle model, where only sigma and the timelike component of the vector mesons were considered, the predicted isoscalar magnetic moments were significantly larger than the observed values [27,28]. This is because the reduced Dirac effective nucleon mass ($M^* \sim 0.6M$) enhances the relativistic effect on the electromagnetic current [29]. It was pointed out that the valence-nucleon approximation is wrong in the relativistic calculation [30].

In reality, however, the current entering the magnetic moment operator is not just the single-particle current of the

*mengj@pku.edu.cn

single valence nucleon. This nucleon polarizes the surrounding medium and this leads to a polarization current induced by the isoscalar current-current interaction. The effective current is therefore reduced. This so-called back-flow effect has been treated in the literature in three different ways. First, the induced current has been calculated in infinite nuclear matter by a Ward identity [31] or in the framework of Landau-Migdal theory [29] and the results have been applied in a local density approximation to finite nuclei. This has been improved by calculating the polarization current in linear response theory in finite spherical systems by summing up the loop diagrams [32–34]. The most direct method, however, is to treat the finite odd-A system in a fully self-consistent way [35–39]. Here the valence nucleon sits in a certain subshell with magnetic quantum number m. This leads to a small axially symmetric deformation and an azimuthal current j_φ around the symmetry axis, which induces in the core a nuclear magnetic field and the corresponding polarization currents. This is all taken into account in a fully self-consistent way by the solution of deformed RMF equations with nuclear magnetic fields breaking time-reversal invariance. For odd-A nuclei in the direct vicinity of an LS closed core, all three methods lead to a strong reduction of the effective current such that the enhancement due to the small effective Dirac mass is nearly canceled and the resulting isoscalar magnetic moments are in excellent with the Schmidt values of the conventional nonrelativistic single-particle model.

Unfortunately, these effects cannot remove the discrepancy existing in isovector magnetic moments. To eliminate this discrepancy, one-pion exchange current corrections have been included in the relativistic model [40,41], and these were found to be significant. However, they lead to a larger disagreement with data. Recently, second-order configuration mixing has been included in the fully self-consistent relativistic theory, and this greatly improves the description of the isovector magnetic moment [42,43].

In Ref. [44] magnetic moments of jj closed-shell ±1 nuclei near ^{208}Pb have been studied in RMF theory including the contribution from the core. The corresponding results show an improvement in comparison with the valence-nucleon approximation. On the other hand, meson exchange currents and configuration mixing, especially first-order configuration mixing, are very important for the description of the magnetic moment of such nuclei.

In view of these facts we present in this manuscript an investigation of magnetic moments of the jj closed-shell ±1 nuclei ^{207}Pb, ^{209}Pb, ^{207}Tl, and ^{209}Bi in a relativistic framework, based on the magnetic moments derived from RMF theory with time-odd fields, including one-pion exchange currents and first- and second-order configuration mixing corrections. For these calculations, the relativistic point-coupling (PC) model will be adopted. In Sec. II we outline briefly the theoretical framework of this model and we present the definition of the magnetic moment operator, the one-pion exchange currents, and configuration mixing diagrams in first and second order. The numerical details are given in Sec. III. The calculations are described and the results are discussed in Sec. IV. Finally, Sec. V contains a brief summary and a perspective.

II. THE RELATIVISTIC FRAMEWORK

A. Relativistic mean field theory

The basic building blocks of RMF theory with point couplings are the vertices

$$(\bar\psi\mathcal{O}\Gamma\psi),\quad \mathcal{O}\in\{1,\vec\tau\},\quad \Gamma\in\{1,\gamma_\mu,\gamma_5,\gamma_5\gamma_\mu,\sigma_{\mu\nu}\},\tag{1}$$

where ψ is the Dirac spinor field, $\vec\tau$ is the isospin Pauli matrix, and Γ generally denotes the 4×4 Dirac matrices. There are 10 such building blocks characterized by their transformation properties in isospin and in Minkowski space. We adopt arrows to indicate vectors in isospin space and bold type for the space vectors. Greek indices μ and ν run over the Minkowski indices 0, 1, 2, and 3.

A general effective Lagrangian can be written as a power series in $\bar\psi\mathcal{O}\Gamma\psi$ and their derivatives. In the present work, we start with the following Lagrangian density [45]:

$$\begin{aligned}\mathcal{L} &= \bar\psi(i\gamma_\mu\partial^\mu - M)\psi - \frac{1}{4}F^{\mu\nu}F_{\mu\nu} - e\frac{1-\tau_3}{2}\bar\psi\gamma^\mu\psi A_\mu\\ &-\frac{1}{2}\alpha_S(\bar\psi\psi)(\bar\psi\psi) - \frac{1}{2}\alpha_V(\bar\psi\gamma_\mu\psi)(\bar\psi\gamma^\mu\psi)\\ &-\frac{1}{2}\alpha_{TV}(\bar\psi\vec\tau\gamma_\mu\psi)(\bar\psi\vec\tau\gamma^\mu\psi)\\ &-\frac{1}{3}\beta_S(\bar\psi\psi)^3 - \frac{1}{4}\gamma_S(\bar\psi\psi)^4 - \frac{1}{4}\gamma_V[(\bar\psi\gamma_\mu\psi)(\bar\psi\gamma^\mu\psi)]^2\\ &-\frac{1}{2}\delta_S\partial_\nu(\bar\psi\psi)\partial^\nu(\bar\psi\psi) - \frac{1}{2}\delta_V\partial_\nu(\bar\psi\gamma_\mu\psi)\partial^\nu(\bar\psi\gamma^\mu\psi)\\ &-\frac{1}{2}\delta_{TV}\partial_\nu(\bar\psi\vec\tau\gamma_\mu\psi)\partial^\nu(\bar\psi\vec\tau\gamma_\mu\psi).\end{aligned}\tag{2}$$

There are nine coupling constants, α_S, α_V, α_{TV}, β_S, γ_S, γ_V, δ_S, δ_V, and δ_{TV}. The subscripts S, V, and T, respectively, indicate the symmetries of the couplings; i.e., S stands for scalar, V for vector, and T for isovector.

Using the mean-field approximation and the "no-sea" approximation, one finds the energy density functional for a nuclear system,

$$E_{\rm DF}[\hat\rho] = \int d^3\boldsymbol{r}\mathcal{E}(\boldsymbol{r}),\tag{3}$$

with the energy density

$$\mathcal{E} = \mathcal{E}_{\rm kin}(\boldsymbol{r}) + \mathcal{E}_{\rm int}(\boldsymbol{r}) + \mathcal{E}_{\rm em}(\boldsymbol{r}),\tag{4}$$

which is composed of a kinetic part,

$$\mathcal{E}_{\rm kin}(\boldsymbol{r}) = \sum_{k=1}^{A}\psi_k^\dagger(\boldsymbol{r})(\boldsymbol{\alpha}\cdot\mathbf{p}+\beta M - M)\psi_k(\boldsymbol{r}),\tag{5}$$

where the sum over k runs over the occupied orbits in the Fermi see (no-sea approximation); an interaction part,

$$\begin{aligned}\mathcal{E}_{\rm int}(\boldsymbol{r}) &= \frac{\alpha_S}{2}\rho_S^2 + \frac{\beta_S}{3}\rho_S^3 + \frac{\gamma_S}{4}\rho_S^4 + \frac{\delta_S}{2}\rho_S\triangle\rho_S\\ &+\frac{\alpha_V}{2}j_\mu j^\mu + \frac{\gamma_V}{4}(j_\mu j^\mu)^2 + \frac{\delta_V}{2}j_\mu\triangle j^\mu\\ &+\frac{\alpha_{TV}}{2}\vec j_{TV}^{\,\mu}\cdot(\vec j_{TV})_\mu + \frac{\delta_{TV}}{2}\vec j_{TV}^{\,\mu}\cdot\triangle(\vec j_{TV})_\mu,\end{aligned}\tag{6}$$

with the local densities and currents

$$\rho_S(\boldsymbol{r}) = \sum_{k=1}^{A} \bar{\psi}_k(\boldsymbol{r})\psi_k(\boldsymbol{r}), \tag{7a}$$

$$j^{\mu}(\boldsymbol{r}) = \sum_{k=1}^{A} \bar{\psi}_k(\boldsymbol{r})\gamma^{\mu}\psi_k(\boldsymbol{r}), \tag{7b}$$

$$\vec{j}^{\mu}_{TV}(\boldsymbol{r}) = \sum_{k=1}^{A} \bar{\psi}_k(\boldsymbol{r})\gamma^{\mu}\vec{\tau}\psi_k(\boldsymbol{r}); \tag{7c}$$

and an electromagnetic part,

$$\mathcal{E}_{\rm em}(\boldsymbol{r}) = \tfrac{1}{4}F_{\mu\nu}F^{\mu\nu} - F^{0\mu}\partial_0 A_{\mu} + eA_{\mu}j^{\mu}_{p}. \tag{8}$$

Minimizing the energy density functional [Eq. (3)] with respect to $\bar{\psi}_k$, one obtains the Dirac equation for the single nucleons,

$$[-i\boldsymbol{\alpha}\cdot\boldsymbol{\nabla} + \beta\gamma_{\mu}V^{\mu} + \beta(M+S)]\psi_k(\boldsymbol{r}) = \varepsilon_k\psi_k(\boldsymbol{r}). \tag{9}$$

The single-particle effective Hamiltonian contains local scalar $S(\boldsymbol{r})$ and vector $V^{\mu}(\boldsymbol{r})$ potentials given by

$$S(\boldsymbol{r}) = \Sigma_S, \quad V^{\mu}(\boldsymbol{r}) = \Sigma^{\mu} + \vec{\tau}\cdot\vec{\Sigma}^{\mu}_{TV}, \tag{10}$$

where the self-energies are given in terms of various densities,

$$\Sigma_S = \alpha_S\rho_S + \beta_S\rho_S^2 + \gamma_S\rho_S^3 + \delta_S\triangle\rho_S, \tag{11a}$$

$$\Sigma^{\mu} = \alpha_V j^{\mu}_V + \gamma_V\left(j^{\mu}_V\right)^3 + \delta_V\triangle j^{\mu}_V + eA^{\mu}, \tag{11b}$$

$$\vec{\Sigma}^{\mu}_{TV} = \alpha_{TV}\vec{j}^{\mu}_{TV} + \delta_{TV}\triangle\vec{j}^{\mu}_{TV}. \tag{11c}$$

For the ground state of an even-even nucleus one has time-reversal symmetry and the spacelike parts of the currents $\boldsymbol{j}(\boldsymbol{r})$ in Eq. (7) as well as the vector potential $\boldsymbol{V}(\boldsymbol{r})$ in Eq. (10), i.e., the time-odd fields, vanish. However, in odd-A nuclei, the odd nucleon breaks the time-reversal invariance, and time-odd fields give rise to a nuclear magnetic potential, which is very important for the description of magnetic moments [35,36]. Moreover, because of charge conservation in nuclei, only the third component of isovector potentials, $\vec{\Sigma}^{\mu}_{TV}$, contributes. The Coulomb field $A_0(\boldsymbol{r})$ is determined by Poisson's equation, and in the applications we neglect the magnetic part $\boldsymbol{A}(\boldsymbol{r})$ of the electromagnetic potential.

The relativistic residual interaction is given by the second derivative of the energy density functional $E(\hat{\rho})$ with respect to the density matrix

$$V_{\alpha\beta\alpha'\beta'} = \frac{\delta^2 E(\hat{\rho})}{\delta\hat{\rho}_{\alpha\beta}\delta\hat{\rho}_{\alpha'\beta'}}. \tag{12}$$

More details can be found in Refs. [46,47].

Although, because of parity conservation, the pion meson does not contribute to the ground state in RMF theory, it plays an important role in spin-isospin excitations and is usually included in relativistic random phase approximation (RPA) and quasi-RPA calculations of these modes [48,49]. The widely used pion-nucleon vertex reads, in its pseudovector coupling form,

$$\mathcal{L}_{\pi N} = -\frac{f_{\pi}}{m_{\pi}}\bar{\psi}\gamma^{\mu}\gamma_5\vec{\tau}\psi\cdot\partial_{\mu}\vec{\pi}, \tag{13}$$

where $\vec{\pi}(\boldsymbol{r})$ is the pion field, f_{π} is the pion-nucleon coupling constant, and m_{π} is the pion mass.

B. The magnetic moment operator

The effective electromagnetic current operator used to describe the nuclear magnetic moment is given by [36–38]

$$\hat{J}^{\mu}(x) = Q\bar{\psi}(x)\gamma^{\mu}\psi(x) + \frac{\kappa}{2M}\partial_{\nu}[\bar{\psi}(x)\sigma^{\mu\nu}\psi(x)], \tag{14}$$

where $Q \equiv \frac{e}{2}(1-\tau_3)$ is the nucleon charge, $\sigma^{\mu\nu} = \frac{i}{2}[\gamma^{\mu},\gamma^{\nu}]$ is the antisymmetric tensor operator, and κ is the free anomalous gyromagnetic ratio of the nucleon: $\kappa_p = 1.793$ and $\kappa_n = -1.913$. In Eq. (14), the first term gives the Dirac current and second term is the so-called anomalous current. The nuclear dipole magnetic moment in units of the nuclear magneton $\mu_N = \frac{e\hbar}{2Mc}$ is determined by

$$\boldsymbol{\mu} = \frac{1}{2\mu_N}\int d^3r\,\boldsymbol{r}\times\langle g.s.|\hat{\boldsymbol{j}}(\boldsymbol{r})|g.s.\rangle \tag{15a}$$

$$= \int d\mathbf{r}\left[\frac{Mc^2}{\hbar c}Q\psi^{+}(\mathbf{r})\mathbf{r}\times\boldsymbol{\alpha}\psi(\mathbf{r}) + \kappa\psi^{+}(\mathbf{r})\beta\boldsymbol{\Sigma}\psi(\mathbf{r})\right], \tag{15b}$$

where $\hat{\boldsymbol{j}}(\boldsymbol{r})$ is the operator of spacelike components of the effective electromagnetic current. The first term in above equation gives the Dirac magnetic moment, and the second term gives the anomalous magnetic moment.

Therefore, in the relativistic theory, the nuclear magnetic moment operator, in units of the nuclear magneton, is given by

$$\hat{\boldsymbol{\mu}} = \frac{Mc^2}{\hbar c}Q\boldsymbol{r}\times\boldsymbol{\alpha} + \kappa\beta\boldsymbol{\Sigma}. \tag{16}$$

C. The one-pion exchange current

Although there is no explicit pion meson in RMF theory, it is possible to study the MEC corrections due to the virtual pion exchange between two nucleons, which, according to Ref. [40], are given by the two Feynman diagrams in Fig. 1.

The one-pion exchange current contributions to magnetic moments are given by

$$\boldsymbol{\mu}_{\rm MEC} = \frac{1}{2}\int d\boldsymbol{r}\,\boldsymbol{r}\times\langle g.s.|\hat{\boldsymbol{j}}^{\rm seagull}(\boldsymbol{r}) + \hat{\boldsymbol{j}}^{\rm in\text{-}flight}(\boldsymbol{r})|g.s.\rangle, \tag{17}$$

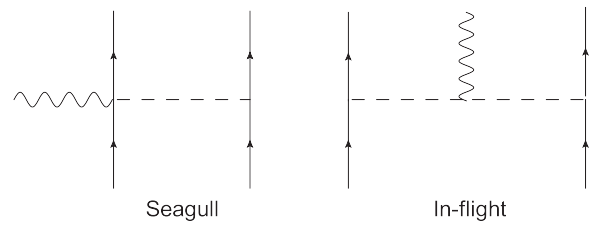

FIG. 1. Diagrams of the one-pion exchange current: seagull (left) and in-flight (right).

with the corresponding one-pion exchange currents $\hat{\boldsymbol{j}}^{\text{seagull}}(\boldsymbol{r})$ and $\hat{\boldsymbol{j}}^{\text{in-flight}}(\boldsymbol{r})$ [41],

$$\hat{\boldsymbol{j}}^{\text{seagull}}(\boldsymbol{r}) = -\frac{8ef_\pi^2 M}{m_\pi^2}\int d\boldsymbol{x}\,\bar{\psi}_p(\boldsymbol{r})\boldsymbol{\gamma}\gamma_5\psi_n(\boldsymbol{r})D_\pi(\boldsymbol{r},\boldsymbol{x})\bar{\psi}_n(\boldsymbol{x}) \times \frac{M^*}{M}\gamma_5\psi_p(\boldsymbol{x}), \tag{18a}$$

$$\hat{\boldsymbol{j}}^{\text{in-flight}}(\boldsymbol{r}) = -\frac{16ief_\pi^2 M^2}{m_\pi^2}\int d\boldsymbol{x}d\boldsymbol{y}\bar{\psi}_p(\boldsymbol{x})\frac{M^*}{M}\gamma_5\psi_n(\boldsymbol{x}) \times D_\pi(\boldsymbol{x},\boldsymbol{r})\nabla_{\boldsymbol{r}}D_\pi(\boldsymbol{r},\boldsymbol{y})\times\bar{\psi}_n(\boldsymbol{y})\frac{M^*}{M}\gamma_5\psi_p(\boldsymbol{y}). \tag{18b}$$

The pion propagator in r space has the form $D_\pi(\boldsymbol{x},\boldsymbol{r}) = \frac{1}{4\pi}\frac{e^{-m_\pi|\boldsymbol{x}-\boldsymbol{r}|}}{|\boldsymbol{x}-\boldsymbol{r}|}$.

D. Configuration mixing

The residual interaction, neglected in the mean-field approximation, leads to configuration mixing, i.e., the coupling between the valence nucleon and particle-hole states in the core. This is also called core polarization. The configuration mixing corrections to the magnetic moment are treated approximately by Rayleigh-Schrödinger perturbation theory.

1. First-order corrections

According to Rayleigh-Schrödinger perturbation theory, the first-order correction to the magnetic moments is determined as

$$\delta\mu_{1\text{st}} = \langle n|\hat{\mu}\frac{\hat{Q}}{E_n-\hat{H}_0}\hat{V}|n\rangle + \langle n|\hat{V}\frac{\hat{Q}}{E_n-\hat{H}_0}\hat{\mu}|n\rangle, \tag{19}$$

where $|n\rangle$ and E_n denote the unperturbed ground-state wave functions and corresponding energies, $\hat{H}_0$ and $\hat{V}$ are the operators of the mean-field Hamiltonian and the residual interaction, respectively, $\hat{\mu}$ is the magnetic moment operator, and $\hat{Q}$ projects onto multiparticle and multihole configurations. The corresponding Feynman diagram is shown in Fig. 2, where the wiggly lines represent the external field (here the magnetic moment operator), and the dashed lines denote the residual interaction. Solid lines with upward arrows denote particle states (i.e., single-particle orbits above the Fermi surface) and those with downward arrows are hole states (i.e., single-particle orbits in the Fermi sea).

For the magnetic moments of nuclei with a doubly closed shell core ±1 nucleon, the formula for the first-order correction can be simplified as

$$\delta\mu_{1\text{st}} = \sum_{j_p j_h J}\frac{2\langle j_h\|\boldsymbol{\mu}\|j_p\rangle}{\Delta E_j}(-1)^{j_h+j+J}\hat{j}^{-1}\sqrt{\frac{j}{j+1}}(2J+1) \times \begin{Bmatrix} j_h & j_p & 1 \\ j & j & J\end{Bmatrix}\langle jj_p;JM|V|jj_h;JM\rangle, \tag{20}$$

where j denotes the valence nucleon state, j_p and j_h represent particle and hole states, and $\Delta E = \varepsilon_{j_p} - \varepsilon_{j_h}$ is the excitation energy of the one-particle–one-hole (1p-1h) excitation. The selection rule $\Delta\ell = 0$ of the nonrelativistic magnetic moment operator allows only particles and holes as spin-orbit partners, i.e., $j_p = \ell - \frac{1}{2}$ and $j_h = \ell + \frac{1}{2}$. All other diagrams vanish. It should be noted that first-order configuration mixing does not provide any contribution in nuclei with an LS closed core ±1 nucleon, because there are no spin-orbit partners on both sides of the Fermi surface and therefore the magnetic-moment operator cannot couple to magnetic resonances [8].

2. Second-order corrections

As shown in Refs. [8,21] the second-order correction to the magnetic moments is given by

$$\delta\mu_{\text{cm}}^{\text{2nd}} = \langle n|\hat{V}\frac{\hat{Q}}{E_n-\hat{H}_0}\hat{\mu}\frac{\hat{Q}}{E_n-\hat{H}_0}\hat{V}|n\rangle - \langle n|\hat{\mu}|n\rangle\langle n|\hat{V}\frac{\hat{Q}}{(E_n-\hat{H}_0)^2}\hat{V}|n\rangle, \tag{21}$$

where the second term comes from the renormalization of the nuclear wave function. In the second-order corrections we have to include one-particle–one-hole and two-particle–two-hole (2p-2h) contributions. As shown in Fig. 3, for a system with a doubly closed shell core, the second-order correction to the magnetic moment can be divided into three terms [8], the contributions of two-particle–one-hole (2p-1h) and of three-particle–two-hole (3p-2h) configurations and of the wave function renormalization, respectively.

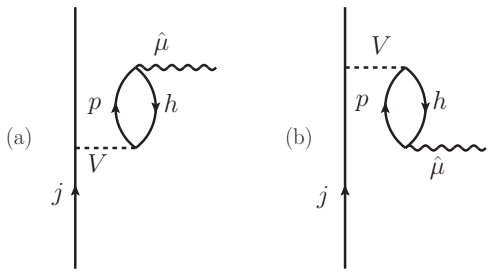

FIG. 2. Diagrams of first-order configuration mixing corrections to the magnetic moment. The external line represents the valence nucleon, and the intermediate particle-hole pair represents an excited state of the core.

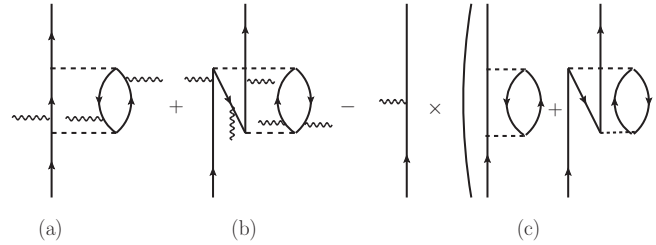

FIG. 3. Diagrams of second-order configuration mixing corrections to the magnetic moment: (a) 1p-1h mode, (b) 2p-2h mode, and (c) wave function renormalization. Diagrams with more than one external wiggly line are an abbreviation for several separate diagrams where each of them has only one wiggly line at the indicated places.

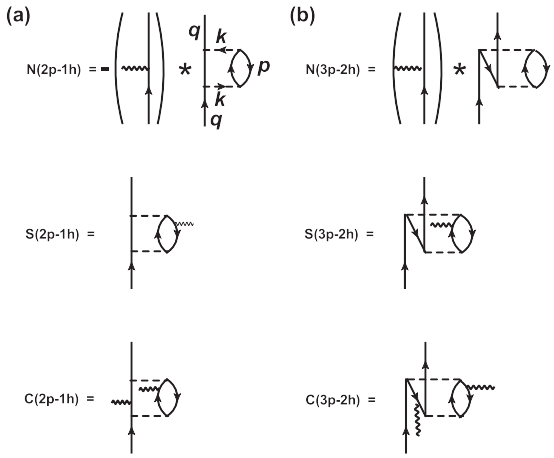

FIG. 4. Diagrams representing second-order configuration mixing corrections: (a) 2p-1h and (b) 3p-2h intermediate states. For the notations N, S, and C, see the text for details.

As shown in Fig. 4, we find for a system with a doubly closed core plus one particle the following second-order corrections to the magnetic moment:

N(2p-1h) and N(3p-2h): from the wave function renormalization,
S(2p-1h) and C(3p-2h): the external field operator acting on the hole line, and
C(2p-1h) and S(3p-2h): the external field operator acting on the particle line,

and we obtain in this case

$$\delta\mu_{\rm cm}^{\rm 2nd} = {\rm N(2p\text{-}1h)} + {\rm S(2p\text{-}1h)} + {\rm C(2p\text{-}1h)} + {\rm N(3p\text{-}2h)} + {\rm S(3p\text{-}2h)} + {\rm C(3p\text{-}2h)}. \quad (22)$$

For a system of a doubly closed core minus one nucleon we have

$$\delta\mu_{\rm cm}^{\rm 2nd} = {\rm N(2h\text{-}1p)} + {\rm S(2h\text{-}1p)} + {\rm C(2h\text{-}1p)} + {\rm N(3h\text{-}2p)} + {\rm S(3h\text{-}2p)} + {\rm C(3h\text{-}2p)}, \quad (23)$$

The detailed formulas for each term can be found in the Appendix.

III. NUMERICAL DETAILS

In this paper we study the magnetic moments of the nuclei ^{207}Pb, ^{209}Pb, ^{207}Tl, and ^{209}Bi. We start on the mean-field level with the magnetic moments derived from RMF theory including time-odd fields and add one-pion exchange currents and first- and second-order configuration mixing contributions. In the calculations, the relativistic point-coupling model with the density functional PC-PK1 [50] is applied.

Spherical RMF theory is solved in coordinate space, with a box size of 15 fm and a step size of 0.1 fm. To calculate the corrections resulting from time-odd fields, triaxially deformed RMF calculations with time-odd fields are performed and each Dirac spinor is expanded in terms of a set of a three-dimensional harmonic oscillator (HO) basis in Cartesian coordinates with 10 major shells [51]. Pairing correlations in the vicinity of the doubly magic nucleus ^{208}Pb are neglected. The one-pion exchange current and configuration mixing corrections to the magnetic moments are calculated using spherical Dirac spinors of the nearby doubly closed shell nucleus ^{208}Pb. The pion-nucleon coupling constant is $f_\pi = 1$ and the pion mass is $m_\pi = 138$ MeV. The configuration mixing corrections depend on the configuration space and this will be discussed in the following applications.

IV. RESULTS AND DISCUSSION

A. First-order corrections

In Table. I we give the first-order configuration mixing corrections to the magnetic moment of ^{209}Bi. They are obtained from relativistic calculations using the density functional PC-PK1 [50] and they are compared with the nonrelativistic results using different interactions: the Kallio-Kolltveit (KK) [52], Gillet [53], Kim-Rasmussen (KR) [54], Brueckner [55], Hamada-Johnston (HJ) [56] and M3Y [57]. The corresponding first-order corrections are taken from Refs. [19,20,58], respectively. For the relativistic calculations, we present results both with and without considering the residual interaction provided by pion exchange.

In nonrelativistic calculations, only the excitations of spin-orbit partners can contribute to the first-order magnetic moment correction, because of selection rules imposed by the magnetic moment single-particle operator. In relativistic calculations this selection rule is only approximately valid. However, in the present relativistic calculations, only two particle-hole excitations can contribute to the first-order magnetic moment correction of ^{209}Bi, i.e., the $(1h_{9/2}1h_{11/2}^{-1})_\pi$ and $(1i_{11/2}1i_{13/2}^{-1})_\nu$ excitations, and all other particle-hole

TABLE I. First-order configuration mixing corrections to the magnetic moment of ^{209}Bi obtained from relativistic calculations using the PC-PK1 effective interaction, in comparison with nonrelativistic results using different interactions. In the relativistic calculations, results both with and without considering the residual interaction provided by the pion are given.

	Nonrelativistic								Relativistic	
Interactions	KK	Gillet	KR I	KR II	Brueckner	HJ	Kuo	M3Y	PC-PK1	PC-PK1
Ref.	[19]			[20,59]			[58]	[57]	without π	with π
$(1h_{9/2}1h_{11/2}^{-1})_\pi$	0.37	0.46	0.53	0.70	0.71	0.55		0.43	−0.11	0.19
$(1i_{11/2}1i_{13/2}^{-1})_\nu$	0.15	−0.02	0.00	−0.06	0.04	0.25		0.24	0.07	0.33
Total	0.52	0.43	0.53	0.64	0.75	0.80	0.79	0.68	−0.04	0.52

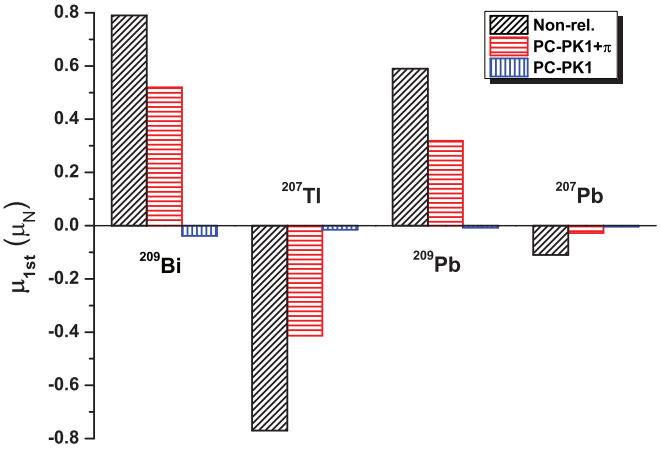

FIG. 5. (Color online) First-order configuration mixing corrections to magnetic moments of ^{209}Bi, ^{207}Tl, ^{209}Pb, and ^{207}Pb obtained from relativistic calculations using the PC-PK1 interaction, in comparison with the nonrelativistic results obtained from Ref. [58]. In the relativistic calculations, the results with and without π are given.

excitations give a small and negligible contribution to its expectation value in first-order perturbation theory.

As shown in Table I the nonrelativistic calculations give remarkable first-order corrections ($0.43\,\mu_N$–$0.80\,\mu_N$), while the corresponding corrections given by relativistic calculations using the PC-PK1 effective interaction are very small ($-0.03\,\mu_N$) and can be neglected. Only after the residual interaction provided by the pion is included does PC-PK1 give significant corrections ($0.59\,\mu_N$) that are consistent with nonrelativistic results.

In order to further confirm the effects of the residual interaction provided by the pion, we show in Fig. 5 the first-order configuration mixing corrections to the magnetic moments of ^{207}Pb, ^{209}Pb, ^{207}Tl, and ^{209}Bi obtained from relativistic calculations using the PC-PK1 interaction. They are compared with nonrelativistic results obtained from Ref. [58]. In Fig. 5 we also see that without the residual interaction provided by the pion, the relativistic calculations give negligible first-order corrections to the magnetic moments of all four nuclei. If the residual interaction provided by the pion is included, relativistic calculations are in reasonable agreement with nonrelativistic results for all present nuclei.

Considering Eq. (20), we find that the magnetic moment operator, the excitation energy, and the interactions can all lead to differences between relativistic and nonrelativistic results. It is well known that the effective mass is relatively small in self-consistent calculations based on density functional theory. This leads to an increased gap at the Fermi surface in the single-particle spectrum and to larger p-h energies. This is a deficiency of conventional density functional theory based on the mean-field approximation with energy-independent self-energies. By taking into account the energy dependence of the self-energy in the framework of couplings to low-lying collective surface modes, considerably larger effective masses and smaller energy gaps have been found in the literature [60–63], and these are closer to the experimental values. Such calculations go, obviously, beyond the scope of the present investigations and therefore we use the experimental single-particle energies rather than the self-consistent RMF single-particle energies in the intermediate states for a relativistic estimation. The experimental excitation energies used in these calculations are $\Delta E_p = \varepsilon(1h_{9/2}) - \varepsilon(1h_{11/2}) = 5.6$ MeV and $\Delta E_n = \varepsilon(1i_{11/2}) - \varepsilon(1i_{13/2}) = 5.86$ MeV. Since the nonrelativistic results are obtained with experimental energy splittings, it is found that, by adopting experimental excitation energy, the relativistic calculations give almost the same first-order corrections as the results by adopting the self-consistent RMF single-particle energies shown in Fig. 5. Although there is some difference between the matrix elements of the relativistic and the nonrelativistic magnetic moment operator, this causes little difference in the first-order corrections in Fig. 5. Therefore, the difference between relativistic and nonrelativistic results are mainly due to interactions, and the residual interaction provided by the pion plays an important role in the relativistic descriptions of nuclear magnetic moments. Therefore it will be included in the following calculations of second-order corrections.

B. Second-order corrections

The theoretical analysis for the Feynman diagrams of second-order configuration mixing shows that the corrections to the magnetic moments are diverging as the configuration space is increased. This is a renormalization problem and it has been shown in detail in the Appendix that the interaction in the point-coupling model is a constant in momentum space and therefore the integrals for the corresponding second-order corrections are diverging. In order to investigate the relationship between second-order corrections and corresponding configuration space, and also to choose the appropriate truncation, the second-order configuration mixing corrections to the magnetic moments of ^{207}Pb, ^{209}Pb, ^{207}Tl, and ^{209}Bi are given in Fig. 6 for major shell truncations [21]; i.e., the configuration space for the calculations of the single-particle

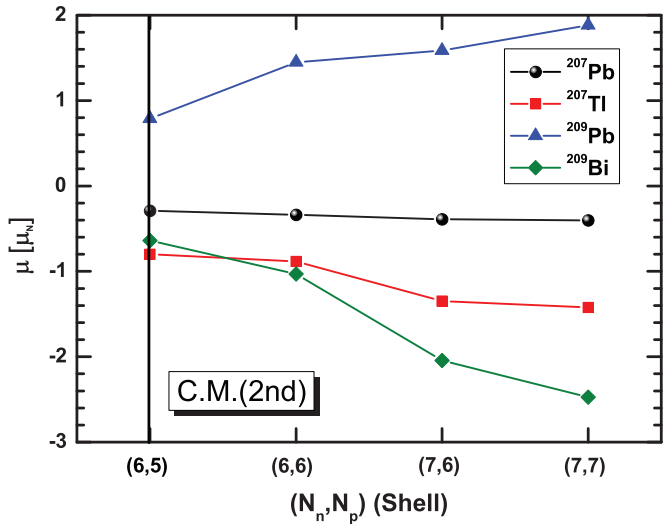

FIG. 6. (Color online) The second-order configuration mixing corrections to the magnetic moments for major shell truncations; i.e., the sum in the intermediate states is restricted to single-particle energies in major shells with the quantum numbers (N_n, N_p).

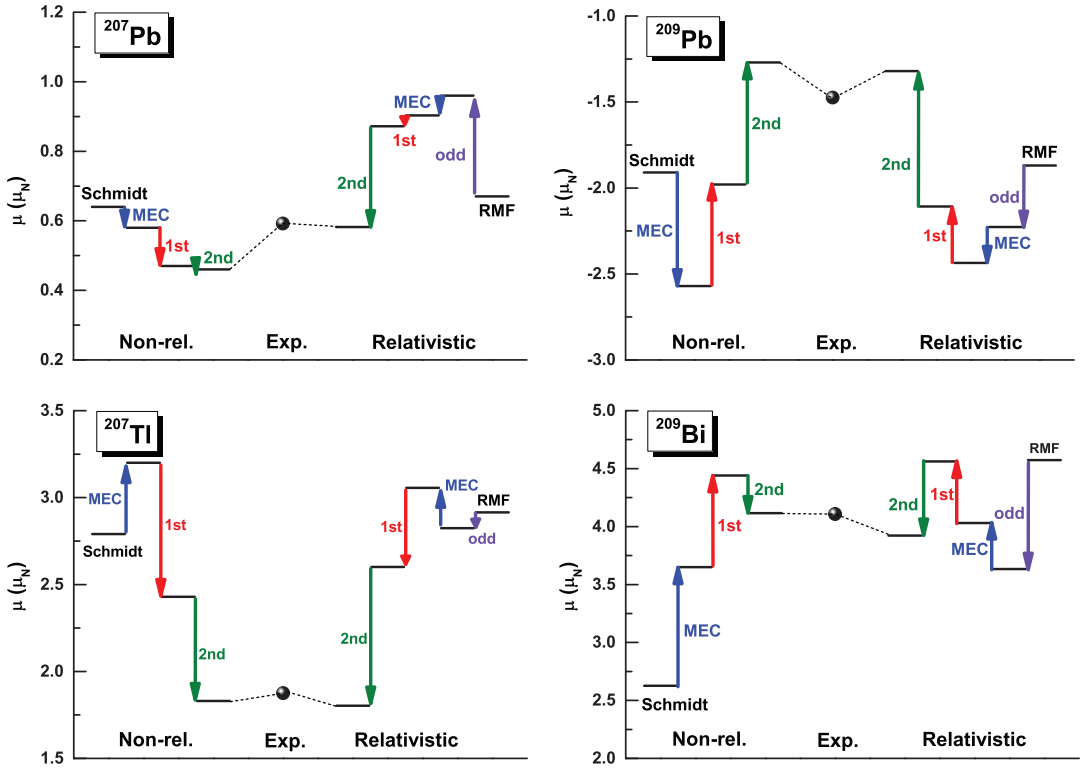

FIG. 7. (Color online) Magnetic moments of the nuclei ^{207}Pb, ^{209}Pb, ^{207}Tl, and ^{209}Bi obtained from relativistic calculations using the PC-PK1 interaction with time-odd contribution, meson exchange currents, and first- and second-order corrections, in comparison with data (solid circles) and the corresponding nonrelativistic results from Ref. [8].

levels in the intermediate states is restricted by the major shells with the quantum numbers $2(n-1)+\ell \leqslant N_n$ for neutrons and $2(n-1)+\ell \leqslant N_p$ for protons, correspondingly.

The second-order corrections of the four nuclei become numerically larger with increasing configuration space. Only the corrections of ^{207}Pb change slightly and vary by 39% from $N_n = 6$, $N_p = 5$ to $N_n = 7$, $N_p = 7$, while the corrections of ^{209}Bi change the most and vary by 287%. This further confirms the divergence for second-order corrections numerically. The present second-order corrections of the four nuclei strongly depend on the orbit of corresponding valence nucleon. In addition, the truncations which give the best descriptions of the present four nuclei are labeled with vertical lines in Fig. 6 ($N_n = 6$, $N_p = 5$, i.e., one major shell above the closed shells with the neutron number $N = 126$ and proton number $Z = 82$). This truncation gives the smallest relative deviations (6.1%) between the relativistic calculations and experimental data, where the relativistic calculations include the magnetic moments from RMF theory, contributions from the corresponding time-odd fields, the one-pion exchange currents, and the first-order as well as second-order corrections. In order to avoid divergent results in perturbation theory a truncation is necessary. The present truncation of one major shell above the closed core is certainly only a first attempt. It is however reasonable, because the important physics takes place in this space. It is also clear that all the nonrelativistic investigations of higher order configuration mixing in the literature are based on finite configuration space. Investigations to treat such diverging diagrams in theories based on density functional theory and going beyond the mean-field concept are in their infancy [64–67].

C. The magnetic moments of nuclei near ^{208}Pb

Figure 7 shows the final results for the magnetic moments of ^{207}Pb, ^{209}Pb, ^{207}Tl, and ^{209}Bi. They are obtained from RMF theory using the density functional PC-PK1 and corresponding corrections are added: time-odd fields (labeled as odd), meson exchange currents (labeled as MEC), and first- (labeled as 1st) and second-order (labeled as 2nd) configuration mixing. The truncation is $2(n-1)+\ell \leqslant 6$ for the neutron level and $2(n-1)+\ell \leqslant 5$ for the proton level. These relativistic results are compared with data (labeled as solid circles) and nonrelativistic results from Ref. [8]. The magnetic moments obtained from spherical RMF theory are labeled as RMF. The differences between magnetic moments of triaxial deformed theory with time-odd fields and magnetic moments of spherical theory represent the corrections due to time-odd fields. In the relativistic calculations, the MEC only contains the one-pion exchange current correction, while the MEC in nonrelativistic calculations includes the one-pion exchange current, the Δ isobar current, and the crossing term between MEC and first-order configuration mixing. For first- and second-order corrections in the relativistic calculation, the residual interaction provided by the poin is included.

It is seen from Fig. 7 that in the relativistic calculations the magnetic moments of all four nuclei are considerably improved by including first-order corrections, MECs, and

second-order corrections, and they are now in agreement with nonrelativistic results. The magnetic moment of ^{207}Pb is excellently reproduced by relativistic calculations, while the corresponding deviation from data is $0.01\,\mu_N$, which is much better than the nonrelativistic deviation of $0.05\,\mu_N$. For ^{209}Pb, the deviations from data are about $0.15\,\mu_N$ and $0.2\,\mu_N$, respectively, for relativistic and nonrelativistic results. For the magnetic moment of ^{207}Tl, both the nonrelativistic description and the relativistic description are very good, as the corresponding two deviations from data are less than $0.1\,\mu_N$. The magnetic moment of ^{209}Bi is also well reproduced by relativistic and nonrelativistic calculations, and the relative deviations from data for both calculations are less than 5%. On the whole, the relative deviation σ_r of the present four nuclei in the relativistic calculation is 6.1%, which is better than the corresponding nonrelativistic results of 13.2% [8].

It is obvious that the first-order, MEC, and second-order corrections given by relativistic calculations have the same sign and order of magnitude as the corresponding corrections given by nonrelativistic calculations. This further shows that the present relativistic calculations, including the appropriate treatment of truncation in second-order corrections, are reasonable.

V. SUMMARY

In summary, by using the relativistic point-coupling model based on the density functional PC-PK1 the magnetic moments of the nuclei ^{209}Pb, ^{207}Pb, ^{209}Bi, and ^{207}Tl with a jj closed-shell core ^{208}Pb are studied, based on the magnetic moments from RMF theory and the corresponding time-odd fields, one-pion exchange current, and first- and second-order corrections. It is found that the second-order diagrams diverge, if the sum over the intermediate single-particle states is carried out to infinity. Therefore a reasonable cutoff is introduced in this sum and only states in the first major shell above the Fermi surface ($N_n = 6$ for neutrons and $N_p = 5$ for protons) are taken into account. The present relativistic calculations are in reasonable agreement with the data. They are compared with corresponding nonrelativistic results from the literature. In general, the relative deviation of 6.1% from experiment for the four nuclei obtained in relativistic calculations is better than the corresponding nonrelativistic results of 13.2%. It is found that the pion is important for describing magnetic moments by means of the one-pion exchange current and by the residual interaction provided by pion exchange.

Of course, there are still many important open questions. So far, we have not included in the configuration mixing calculations the contributions of the Dirac sea, because they are far from the configurations space under consideration. It remains to consider them in more detail in future investigations. We also have neglected, so far, the crossing terms between the MEC and configuration mixing as well as the influence of higher order diagrams in RPA-type configuration mixing calculations [68]. An additional point not included so far is the coupling to the Δ isobar current [69–71]. Of course, it will be also interesting to study the influence of other successful covariant density functionals on the market, in particular those based on relativistic Hartree-Fock theory [72], where the pion and the resulting tensor forces can be included in a self-consistent way. Work in this direction is in progress.

One of the major results of this investigation is the fact that there are essential limitations for extensions of density functional theory going beyond the mean-field concept. Nearly all extensions based on perturbation theory show divergences for zero-range forces in specific diagrams [61]. It is evident that this cannot be treated by just replacing the zero-range force by finite-range forces, as for instance by replacing the point-coupling models with finite-range meson exchange models, because it all depends on the range. For heavy mesons this range is very short and this leads to very large and unphysical corrections [73]. In the past one has avoided this problem by restriction to relatively small valence spaces often dictated by computational limitations (in shell-model configuration mixing calculations) and additional parameters in the form of effective charges often chosen in a very arbitrary way. The investigation presented here uses a similar concept, allowing only one major shell above the Fermi surface for the configuration mixing.

A renormalization seems to be necessary. In the past, specific renormalization recipes have been employed successfully for specific cases, as in the calculation of the fragmentation of single-particle levels by particle vibrational couplings [60], in the problem of pairing with zero-range forces [74], or in extended linear response calculations with energy-dependent effective interactions [75]. Of course, in future, a more systematic renormalization procedure seems to be desirable. First investigations in this direction are in their infancy [65–67].

ACKNOWLEDGMENTS

We would like to thank Akito Arima, Haozhao Liang, and Jiangming Yao for discussions and collaboration. This work is partly supported by the Major State 973 Program 2013CB834400, the NSFC (Grants No. 11335002, No. 11175002, and No. 11205068), the Research Fund for the Doctoral Program of Higher Education (Grant No. 20110001110087), CPSC (Grants No. 2012M520100 and No. 2012M520667), and the DFG cluster of excellence "Origin and Structure of the Universe" (www.universe-cluster.de).

APPENDIX A: SECOND-ORDER CORRECTIONS

In the second-order correction, both 1p-1h and 2p-2h excitation modes can be divided into three parts, N, S, and C, respectively [8,21],

$$\mathrm{N} = \mp\langle j|\hat{\mu}|j\rangle\langle j|V\frac{\hat{Q}}{\left(E_j^{(0)}-\hat{H}_0\right)^2}V|j\rangle, \tag{A1a}$$

$$\mathrm{S} = \langle j|V\frac{\hat{Q}}{E_j^{(0)}-\hat{H}_0}\hat{\mu}\frac{Q}{E_j^{(0)}-\hat{H}_0}V|j\rangle, \tag{A1b}$$

$$\mathrm{C} = \langle j|V\frac{\hat{Q}}{E_j^{(0)}-\hat{H}_0}\hat{\mu}\frac{Q}{E_j^{(0)}-\hat{H}_0}V|j\rangle. \tag{A1c}$$

In Eq. (A1a), the minus sign (−) is for the 1p-1h mode and the plus sign (+) is for the 2p-2h mode. For the nuclei of doubly

closed shells plus one nucleon, the corresponding second-order correction can be written as

$$\mathrm{N(2p\text{-}1h)} = -\langle j\|\boldsymbol{\mu}\|j\rangle \sum_{j_1 j_2 j_h, J} \frac{\hat{J}^2 \hat{j}^{-2}}{\Delta E_j^2} \langle jj_h, J|V|j_1 j_2, J\rangle^2, \tag{A2a}$$

$$\begin{aligned}\mathrm{S(2p\text{-}1h)} = &-\sum_{j_h j_{h'}} \sum_{j_1 j_2, J} (-1)^{j_{h'}+J+j} \hat{J}^2 \begin{Bmatrix} j_h & j_{h'} & 1 \\ j & j & J \end{Bmatrix} \\ &\times \frac{1}{\Delta E \Delta E'} \langle j_{h'}\|\boldsymbol{\mu}\|j_h\rangle \langle jj_h, J|V|j_1 j_2, J\rangle \\ &\times \langle j_1 j_2, J|V|jj_{h'}, J\rangle, \end{aligned} \tag{A2b}$$

$$\begin{aligned}\mathrm{C(2p\text{-}1h)} = &\sum_{j_1 j_2, j_1' j_h} \sum_{JJ'} (-1)^{j_1+j_2+j_h+j} 2\hat{J}^2 \hat{J}'^2 \langle j_1\|\boldsymbol{\mu}\|j_1'\rangle \\ &\times \begin{Bmatrix} J & 1 & J' \\ j_1' & j_2 & j_1 \end{Bmatrix} \begin{Bmatrix} J' & 1 & J \\ j & j_h & j \end{Bmatrix} \frac{1}{\Delta E \Delta E'} \\ &\times \langle jj_h, J|V|j_1 j_2, J\rangle \langle j_1' j_2, J'|V|jj_h, J'\rangle, \end{aligned} \tag{A2c}$$

$$\mathrm{N(3p\text{-}2h)} = -\langle j\|\boldsymbol{\mu}\|j\rangle \sum_{j_{h_1} j_{h_2}}^{j_1, J} \frac{\hat{J}^2 \hat{j}^{-2}}{\Delta E_j^2} \langle jj_1, J|V|j_{h_1} j_{h_2}, J\rangle^2, \tag{A2d}$$

$$\begin{aligned}\mathrm{S(3p\text{-}2h)} = &-\sum_{j_{h_1} j_{h_2}} \sum_{j_1 j_2, J} \frac{(-1)^{j_1+J+j} \hat{J}^2}{\Delta E \Delta E'} \begin{Bmatrix} j_1 & j_2 & 1 \\ j & j & J \end{Bmatrix} \\ &\times \langle j_1\|\boldsymbol{\mu}\|j_2\rangle \langle jj_1, J|V|j_{h_1} j_{h_2}, J\rangle \\ &\times \langle j_{h_1} j_{h_2}, J|V|jj_2, J\rangle, \end{aligned} \tag{A2e}$$

$$\begin{aligned}\mathrm{C(3p\text{-}2h)} = &\sum_{j_{h_1} j_{h_2} j_{h_1'}} \sum_{j_1 JJ'} (-1)^{j_{h_1}+j_{h_2}+j_1+j} \langle j_{h_1}\|\boldsymbol{\mu}\|j_{h_1'}\rangle \\ &\times \frac{2\hat{J}^2 \hat{J}'^2}{\Delta E \Delta E'} \begin{Bmatrix} J & 1 & J' \\ j_{h_1'} & j_{h_2} & j_{h_1} \end{Bmatrix} \begin{Bmatrix} J' & 1 & J \\ j & j_1 & j \end{Bmatrix} \\ &\times \langle jj_1, J|V|j_{h_1} j_{h_2}, J\rangle \langle j_{h_1'} j_{h_2}, J'|V|jj_1, J'\rangle. \end{aligned} \tag{A2f}$$

All formulas should be accompanied by a factor $\langle jj10|jj\rangle/\sqrt{2j+1}$. ΔE is the excitation energy of the 2p-1h (3p-2h) immediate states. For nuclei with one hole, the formulas for $N(2\mathrm{h}-1\mathrm{p})$ etc. are simply given by interchanging the indices p and h.

Some Feynman diagrams [76] for second-order corrections are not convergent. This can easily be seen in momentum space. If we take the term N(2p-1h) as an example, the Feynman diagram (shown in Fig. 4) corresponds to the following integration:

$$\mathrm{N(2p-1h)} = -\langle j||\hat{\mu}||j\rangle \int_\Gamma \frac{d^3K}{(2\pi)^3} \frac{d^3P}{(2\pi)^3} |V_K|^2 \frac{1}{\Delta E^2}, \tag{A3}$$

where the integration space Γ includes $|P|<k_F$, $|P+K|>k_F$, and $|q+K|>k_F$, and q, K, and P denote the momentum of the valence nucleon, the exchange momentum between the valence nucleon and the 1p-1h bubble, and the momentum of hole state, respectively. In the small or large momentum transform limit ($K\to 0$ or $K\to\infty$), the excited energy of the intermediate state is $\Delta E = \varepsilon_{q-K} + \varepsilon_{P+K} - \varepsilon_P - \varepsilon_q \sim K$. In the point-coupling model, V_K is a constant and therefore

$$\mathrm{N(2p-1h)} \sim \int d^3K \frac{1}{K^2} \cdots. \tag{A4}$$

Since $|q+K|>k_F$, K can be infinite. Therefore, the N(2p-1h) term diverges.

After a similar analysis of the other terms, we found that for a nucleus with a core plus one nucleon (hole), the terms with 2p-1h (3h-2p) intermediate states are not convergent either. The easiest way to deal with this divergence is to introduce an appropriate truncation in the integration space.

APPENDIX B: THE RESIDUAL INTERACTION IN THE RELATIVISTIC POINT-COUPLING MODEL

As noted in Eq. (12), the relativistic residual interaction is determined by the second derivative of the energy density functional with respect to the density matrix. It can be expressed as $V^i_{\alpha\beta\alpha'\beta'} = \langle\alpha\beta|V^i|\alpha'\beta'\rangle$, with

$$\begin{aligned} V^S &= \gamma_0(1)(\alpha_S + 2\beta_S\rho_S + 3\gamma_S\rho_S^2 + \delta_S\Delta)_1\, \gamma_0(2) \\ &\quad\times \delta(\boldsymbol{r}_1 - \boldsymbol{r}_2), \end{aligned} \tag{B1}$$

$$\begin{aligned} V^V &= \left\{\left[\alpha_V + 3\gamma_V\rho_V^2 + \delta_V\Delta\right]_1 - \boldsymbol{\alpha}(1)[\alpha_V + \gamma_V\rho_V^2 \right. \\ &\quad \left. + \delta_V\Delta]_1\boldsymbol{\alpha}(2)\right\} \times \delta(\boldsymbol{r}_1 - \boldsymbol{r}_2), \end{aligned} \tag{B2}$$

$$V^{TV} = [\gamma_0\gamma_\mu(\alpha_{TV} + \delta_{TV}\Delta)\vec{\tau}]_1\, [\gamma_0\gamma^\mu\vec{\tau}]_2\, \delta(\boldsymbol{r}_1 - \boldsymbol{r}_2), \tag{B3}$$

$$V^C = \frac{e^2}{4}[\gamma_0\gamma_\mu(1-\tau_3)]_1[\gamma_0\gamma^\mu(1-\tau_3)]_2, \tag{B4}$$

which are for isoscalar, vector, isovector-vector, and Coulomb interactions, respectively.

With the pion-nucleon Lagrangian density in Eq. (13), the corresponding interaction reads

$$V^\pi = -\left[\frac{f_\pi}{m_\pi}\vec{\tau}\gamma_0\gamma_5\gamma^k\partial_k\right]_1 \cdot \left[\frac{f_\pi}{m_\pi}\vec{\tau}\gamma_0\gamma_5\gamma^l\partial_l\right]_2 D_\pi(1,2). \tag{B5}$$

In order to cancel the contact interaction coming from the pion pseudovector coupling, one includes a zero-range pionic counterterm, which reads

$$V^{\pi\delta} = \frac{1}{3}\left[\frac{f_\pi}{m_\pi}\vec{\tau}\gamma_0\gamma_5\boldsymbol{\gamma}\right]_1 \cdot \left[\frac{f_\pi}{m_\pi}\vec{\tau}\gamma_0\gamma_5\boldsymbol{\gamma}\right]_2 \delta(\boldsymbol{r}_1 - \boldsymbol{r}_2). \tag{B6}$$

[1] R. J. Blin-Stoyle, Rev. Mod. Phys. **28**, 75 (1956).
[2] A. Arima, Prog. Part. Nucl. Phys. **11**, 53 (1984).
[3] B. Castel and I. S. Towner, *Modern Theories of Nuclear Moments* (Clarendon, Oxford, 1990).
[4] I. Talmi, Int. J. Mod. Phys. E **14**, 821 (2005).
[5] R. J. Blin-Stoyle, Proc. Phys. Soc. A **66**, 1158 (1953).
[6] T. Schmidt, Z. Phys. **106**, 358 (1937).
[7] I. S. Towner, Phys. Rep. **155**, 263 (1987).

[8] A. Arima, K. Shimizu, W. Bentz, and H. Hyuga, Adv. Nucl. Phys. **18**, 1 (1987).
[9] A. Arima, Sci. China Phys. Mech. Astron. **54**, 188 (2011).
[10] A. Arima and H. Horie, Prog. Theor. Phys. **11**, 509 (1954).
[11] I. Talmi, J. Phys. Conf. **20**, 28 (2005).
[12] A. Arima and H. Horie, Prog. Theor. Phys. **12**, 623 (1954).
[13] N. Hiroshi, A. Arima, and H. Horie, Prog. Theor. Phys. Suppl. **8**, 33 (1958).
[14] H. Miyazawa, Prog. Theor. Phys. **6**, 801 (1951).
[15] F. Villars, Phys. Rev. **86**, 476 (1952).
[16] M. Chemtob, Nucl. Phys. A **123**, 449 (1969).
[17] H. Hyuga, A. Arima, and K. Shimizu, Nucl. Phys. A **336**, 363 (1980).
[18] M. Ichimura and K. Yazaki, Nucl. Phys. **63**, 401 (1965).
[19] H. A. Mavromatis, L. Zamick, and G. E. Brown, Nucl. Phys. **80**, 545 (1966).
[20] H. A. Mavromatis and L. Zamick, Nucl. Phys. A **104**, 17 (1967).
[21] K. Shimizu, M. Ichimura, and A. Arima, Nucl. Phys. A **226**, 282 (1974).
[22] I. S. Towner and F. C. Khanna, Nucl. Phys. A **399**, 334 (1983).
[23] P. G. Reinhard, Rep. Prog. Phys. **52**, 439 (1989).
[24] P. Ring, Prog. Part. Nucl. Phys. **37**, 193 (1996).
[25] D. Vretenar, A. Afanasjev, G. Lalazissis, and P. Ring, Phys. Rep. **409**, 101 (2005).
[26] J. Meng, H. Toki, S. Zhou, S. Zhang, W. Long, and L. Geng, Prog. Part. Nucl. Phys. **57**, 470 (2006).
[27] L. D. Miller, Ann. Phys. (NY) **91**, 40 (1975).
[28] B. D. Serot, Phys. Lett. B **107**, 263 (1981).
[29] J. A. McNeil, R. D. Amado, C. J. Horowitz, M. Oka, J. R. Shepard, and D. A. Sparrow, Phys. Rev. C **34**, 746 (1986).
[30] B. D. Serot, Rep. Prog. Phys. **55**, 1855 (1992).
[31] W. Bentz, A. Arima, H. Hyuga, K. Shimizu, and K. Yazaki, Nucl. Phys. A **436**, 593 (1985).
[32] S. Ichii, W. Bentz, A. Arima, and T. Suzuki, Phys. Lett. B **192**, 11 (1987).
[33] J. R. Shepard, E. Rost, C.-Y. Cheung, and J. A. Mc Neil, Phys. Rev. C **37**, 1130 (1988).
[34] R. J. Furnstahl, Phys. Rev. C **38**, 370 (1988).
[35] U. Hofmann and P. Ring, Phys. Lett. B **214**, 307 (1988).
[36] R. J. Furnstahl and C. E. Price, Phys. Rev. C **40**, 1398 (1989).
[37] J. M. Yao, H. Chen, and J. Meng, Phys. Rev. C **74**, 024307 (2006).
[38] J. Li, Y. Zhang, J. M. Yao, and J. Meng, Sci. China Ser. G **52**, 1586 (2009).
[39] J. Li, J. M. Yao, and J. Meng, Chin. Phys. C **33**, 98 (2009).
[40] T. M. Morse, C. E. Price, and J. R. Shepard, Phys. Lett. B **251**, 241 (1990).
[41] J. Li, J. M. Yao, J. Meng, and A. Arima, Prog. Theor. Phys. **125**, 1185 (2011).
[42] J. Li, J. Meng, P. Ring, J. M. Yao, and A. Arima, Sci. China Phys. Mech. Astron. **54**, 204 (2011).
[43] J. Wei, J. Li, and J. Meng, Prog. Theor. Phys. Suppl. **196**, 400 (2012).
[44] R. J. Furnstahl and S. Brian D., Nucl. Phys. A **468**, 539 (1987).
[45] T. Büvenich, D. G. Madland, J. A. Maruhn, and P.-G. Reinhard, Phys. Rev. C **65**, 044308 (2002).
[46] T. Nikšić, D. Vretenar, and P. Ring, Phys. Rev. C **72**, 014312 (2005).
[47] J. Daoutidis and P. Ring, Phys. Rev. C **80**, 024309 (2009).
[48] C. De Conti, A. P. Galeão, and F. Krmpotić, Phys. Lett. B **444**, 14 (1998).
[49] N. Paar, T. Nikšić, D. Vretenar, and P. Ring, Phys. Rev. C **69**, 054303 (2004).
[50] P. W. Zhao, Z. P. Li, J. M. Yao, and J. Meng, Phys. Rev. C **82**, 054319 (2010).
[51] W. Koepf and P. Ring, Nucl. Phys. A **493**, 61 (1989).
[52] A. M. Green, A. Kallio, and K. Kolltveit, Phys. Lett. **14**, 142 (1965).
[53] V. Gillet, A. M. Green, and E. A. Sanderson, Phys. Lett. **11**, 44 (1964).
[54] Y. E. Kim and J. O. Rasmussen, Nucl. Phys. **47**, 184 (1963).
[55] K. A. Brueckner and J. L. Gammel, Phys. Rev. **109**, 1023 (1958).
[56] T. Hamada and I. D. Johnston, Nucl. Phys. **34**, 382 (1962).
[57] G. Bertsch, J. Borysowicz, H. McManus, and W. G. Love, Nucl. Phys. A **284**, 399 (1977).
[58] A. Arima and L. J. Huang-Lin, Phys. Lett. B **41**, 435 (1972).
[59] J. Blomqvist, N. Freed, and H. O. Zetterström, Phys. Lett. **18**, 47 (1965).
[60] P. Ring and E. Werner, Nucl. Phys. A **211**, 198 (1973).
[61] V. Bernard and N. Van Giai, Nucl. Phys. A **348**, 75 (1980).
[62] E. Litvinova and P. Ring, Phys. Rev. C **73**, 044328 (2006).
[63] P. Ring and E. Litvinova, Phys. At. Nucl. **72**, 1285 (2009).
[64] E. Litvinova, P. Ring, and V. Tselyaev, Phys. Rev. C **75**, 064308 (2007).
[65] K. Moghrabi, M. Grasso, G. Colò, and N. Van Giai, Phys. Rev. Lett. **105**, 262501 (2010).
[66] K. Moghrabi, M. Grasso, X. Roca-Maza, and G. Colò, Phys. Rev. C **85**, 044323 (2012).
[67] K. Moghrabi and M. Grasso, Phys. Rev. C **86**, 044319 (2012).
[68] R. Bauer, J. Speth, V. Klemt, P. Ring, E. Werner, and T. Yamazaki, Nucl. Phys. A **209**, 535 (1973).
[69] M. Rho, Nucl. Phys. A **231**, 493 (1974).
[70] E. Oset and M. Rho, Phys. Rev. Lett. **42**, 47 (1979).
[71] W. Knüpfer, M. Dillig, and A. Richter, Phys. Lett. B **95**, 349 (1980).
[72] W.-H. Long, N. Van Giai, and J. Meng, Phys. Lett. B **640**, 150 (2006).
[73] H. Kucharek and P. Ring, Z. Phys. A **339**, 23 (1991).
[74] J. Dobaczewski, W. Nazarewicz, T. R. Werner, J. F. Berger, C. R. Chinn, and J. Dechargé, Phys. Rev. C **53**, 2809 (1996).
[75] V. I. Tselyaev, Phys. Rev. C **75**, 024306 (2007).
[76] R. D. Mattuck, *A Guide to Feynman Diagrams in the Many-Body Problem* (Dover, New York, 1992).